IOPscience iopscience.iop.org

Home Search Collections Journals About Contact us My IOPscience

Electromagnetically induced angular Talbot effect

This content has been downloaded from IOPscience. Please scroll down to see the full text.

2015 J. Phys. B: At. Mol. Opt. Phys. 48 245502

(http://iopscience.iop.org/0953-4075/48/24/245502)

View the table of contents for this issue, or go to the journal homepage for more

Download details:

IP Address: 153.90.170.23
This content was downloaded on 28/03/2017 at 06:47

Please note that terms and conditions apply.

You may also be interested in:

Electromagnetically induced second-order Talbot effect
Tianhui Qiu, Guojian Yang and Qing Bian

Two-dimensional electromagnetically induced grating via gain and phase modulation in two-level system
Guang-Ling Cheng, Lu Cong and Ai-Xi Chen

Two-dimensional electromagnetically induced cross-grating in a four-level N-type atomic system
Jianchun Wu and Baoquan Ai

Two-dimensional electromagnetically induced grating in coherent atomic medium
Yuyuan Chen, Zhuanzhuan Liu and Rengang Wan

Electromagnetically induced grating in a three-level \Xi-type system
Bibhas K Dutta and Prasanta K Mahapatra

Two-dimensional electromagnetically induced cross-grating in a four-level tripod-type atomic system
Li Wang, Fengxue Zhou, Pidong Hu et al.

Phase grating in a doubly degenerate four-level system
Liu Yun, Wang Pu and Peng Shuang-Yan

Electromagnetically induced grating in a four-level tripod-type atomic system
Dong Ya-Bin and Guo Yao-Hua

Investigation of dual electromagnetically induced grating based on spatial modulation in quantum well nanostructures via biexciton coherence
Tayebeh Naseri

IOP Publishing Journal of Physics B: Atomic, Molecular and Optical Physics
J. Phys. B: At. Mol. Opt. Phys. **48** (2015) 245502 (7pp) doi:10.1088/0953-4075/48/24/245502

Electromagnetically induced angular Talbot effect

Tianhui Qiu[1] **and Guojian Yang**[2]

[1] School of Science, Qingdao Technological University, Qingdao 266033, People's Republic of China
[2] Department of Physics, and Applied Optics Beijing Area Major Laboratory, Beijing Normal University, Beijing 100875, People's Republic of China

E-mail: yanggj@bnu.edu.cn

Received 9 June 2015, revised 6 September 2015
Accepted for publication 21 September 2015
Published 28 October 2015

Abstract

The discrete angular spectrum (angular Talbot effect) of a periodic grating illuminated by a suitable spherical wave front has been observed recently (Azaña and Chatellus 2104 *Phys. Rev. Lett.* **112** 213902). In this paper we study the possibility of such a phenomenon being realized with a medium that has no macroperiodic structure itself. Tunable electromagnetically induced grating (EIG) could be such a kind of medium. We obtain an EIG based on the periodically modulated strong susceptibility due to the third-order nonlinear effect generated in a double Λ-type four-level atomic system, and show the angular Talbot effect of an amplitude EIG, as well as a hybrid EIG, as the condition of the discrete phase-modulation shift of the illumination light front is satisfied. EIG parameters are tunable and the EIG-based angular Talbot effect may have the same potential applications as its periodic grating counterpart has.

Keywords: electromagnetically induced transparency, angular Talbot effect, third-order nonlinear

1. Introduction

The Talbot effect is a phenomenon in which the self-imaging of a periodic object occurs repeatedly at specific locations without using a lens or any other optical elements between the object and its images [1]. Physically, it is a near-field diffraction effect. Last year, José Azaña *et al* showed integer and fractional self-imaging effects or angular spectra of a grating, i.e., a kind of far-field diffraction phenomenon, with a suitable parabolic wave front illumination, and referred to this new effect as the 'angular Talbot phenomenon' [2]. Since the self-imaging effect was first reported in 1836 by Henry Fox Talbot [1], the Talbot effect has attracted much attention in both theoretical and experimental fields. This is due to its important applications in image processing and synthesis, photolithography, optical testing, optical metrology, and spectrometry [3]. Self-imaging has also been demonstrated in atomic waves [4, 5], Bose–Einstein condensates [6], large C_{70} fullerene molecules [7], x-ray phase imaging [8, 9], and so on.

Investigations into self-imaging are mostly devoted to an imaged object which must have periodic structure. Two years ago, Xiao *et al* proposed a scheme where the self-imaging was realized with the imaged object without periodic structure itself. This scheme is so called the electromagnetically induced Talbot effect (EITE) [10]. The object to be imaged is an electromagnetically induced grating (EIG) [11–13], an optical-material complex, where the object is composed of ultracold atoms or molecules in homogenous distribution and couples with a strong standing wave. An EIG acts as a grating because of its capacity of periodically modulating the optical response of the medium to a weak illumination field based on the electromagnetically induced transparency (EIT) [14]. So far, the study of EITE has been extended from its first-order light correlation case [10] to its second-order counterpart [15]. Apart from the potential applications that the conventional Talbot self-imaging effects are predicted to have, the EITE technique may provide a new option for imaging ultracold atoms or molecules [10].

The EIT related optical effects described above originate from the linear optical response of matter to light. In some cases, however, this linear restriction could be released, and the nonlinear susceptibilities are very large even if the linear susceptibility vanishes. So far there have been many interesting observations about the optical phenomena based on EIT determined by nonlinear susceptibility [16–19]. In this paper, we propose a scheme for the angular Talbot effect of

 © 2015 IOP Publishing Ltd Printed in the UK

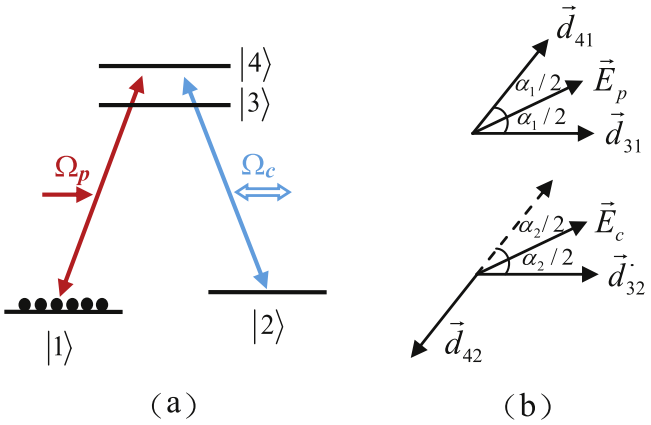

Figure 1. (a) Schematic diagram of atom–field interaction, (b) arrangement of probe field ($\vec{E}_p$) and control field ($\vec{E}_c$), and the relevant dipole moments.

an EIG, i.e., the electromagnetically induced angular Talbot effect (EIATE). Here the EIG results from the strong third-order susceptibility instead of the first-order one, periodically modulated by a standing wave. Specifically, the scheme to be considered is a double Λ-type four-level system, where the sufficient nonlinearity results from inherent quantum interference between the different atomic decay channels, so there is no need for the additional strong coupling fields that a conventional scheme of strong nonlinearity generation requires. We find that the periodically modulated nonlinear susceptibility can lead to a pure amplitude or a hybrid EIG and also the self-imaging effect of the EIG in the far-field diffraction regime.

2. Model of atom–photon interaction

The model under consideration is shown in figure 1(a). There is a double Λ-type four-level atomic system with z-direction length L. Its two closely lying excited states $|3\rangle$ and $|4\rangle$ separated by a frequency difference 2Δ are collectively coupled to the level $|1\rangle$ via a probe field with frequency $\omega_{\rm p}$, amplitude $E_{\rm p}$ and associated Rabi frequencies $\Omega_{\rm p1}=E_{\rm p}d_{31}/2\hbar$ and $\Omega_{\rm p2}=E_{\rm p}d_{41}/2\hbar$, and to the level $|2\rangle$ via a strong control field with frequency ω_c, amplitude $E_{\rm c}$ and associated Rabi frequencies $\Omega_{\rm c1}=E_{\rm c}d_{32}/2\hbar$ and $\Omega_{\rm c2}=E_{\rm c}d_{42}/2\hbar$, respectively. Here, d_{ij} is the electric-dipole moment of transition $|i\rangle\leftrightarrow|j\rangle$. The probe field propagates in the z-direction and its amplitude $E_{\rm p}$ is x-dependent. For simplicity, we assume in the following that $d_{4i}/d_{3i}=g_i$ and the misalignment angle α_i between $\vec{d}_{3i}$ and $\vec{d}_{4i}$ $(i=1,2)$ is equally divided by $\vec{E}_{\rm p}$ for $(i=1)$ or $\vec{E}_{\rm c}$ for $(i=2)$, which is shown in figure 1(b). Then we have $\Omega_{\rm p1}=\Omega_{\rm p2}/g_{\rm l}=\Omega_{\rm p}$ and $\Omega_{\rm c1}=\Omega_{\rm c2}/g_2=\Omega_{\rm c}$.

Based on the Weisskopf–Wigner theory, we can obtain the following dynamical equations of the atomic probability amplitude $a_i(t)$ in state $|i\rangle$ under the electric-dipole and the rotating-wave approximations:

$$\begin{aligned}
\frac{\partial a_1}{\partial t}&=i\Omega_{\rm p1}^{*}a_3+ig_{\rm l}\Omega_{\rm p1}^{*}a_4,\\
\frac{\partial a_2}{\partial t}&=i\big(\Delta_{\rm p}-\Delta_{\rm c}\big)a_2-\gamma_{21}a_2+i\Omega_{\rm c1}^{*}a_3+ig_2\Omega_{\rm c1}^{*}a_4,\\
\frac{\partial a_3}{\partial t}&=i\big(\Delta_{\rm p}+\Delta\big)a_3-\frac{\Gamma_{31}+\Gamma_{32}}{2}a_3+i\Omega_{\rm p1}a_1\\
&\quad+i\Omega_{\rm c1}a_2-\gamma_{43}a_4,\\
\frac{\partial a_4}{\partial t}&=i\big(\Delta_{\rm p}-\Delta\big)a_4-\frac{\Gamma_{41}+\Gamma_{42}}{2}a_4+ig_{\rm l}\Omega_{\rm p1}a_1\\
&\quad+ig_2\Omega_{\rm c1}a_2-\gamma_{43}a_3,
\end{aligned}\tag{1}$$

where Γ_{ij} is the spontaneous decay rate from the state $|i\rangle$ to $|j\rangle$, and γ_{21} is the dephasing rate of the atomic spin excitation. $\Delta_{\rm p}=\omega_{\rm p}-(\omega_{31}+\omega_{41})/2$ and $\Delta_{\rm c}=\omega_{\rm c}-(\omega_{32}+\omega_{42})/2$ are the detunings of the probe and the control fields, respectively. In addition, $\gamma_{43}=(p_1\sqrt{\Gamma_{31}\Gamma_{41}}+p_2\sqrt{\Gamma_{32}\Gamma_{42}})/2$ with $p_i=\vec{d}_{3i}\cdot\vec{d}_{4i}/|\vec{d}_{3i}||\vec{d}_{4i}|=\cos\alpha_i$, here the term $p_i\sqrt{\Gamma_{3i}\Gamma_{4i}}$ describes the inherent quantum interference resulting from the cross coupling between spontaneous decay pathways $|3\rangle\rightarrow|i\rangle$ and $|4\rangle\rightarrow|i\rangle$ $(i=1,2)$ [20–22]. We note here that the requirement of an atom with the structure available for generating inherent quantum interference is that this atom should have a near-degenerate level structure with nonorthogonal dipoles. However, it is not easy to find this atomic structure in nature. This kind of problem can be solved in the dressed-state picture of a coherently driven atomic system.

Assuming that all the atoms are initially prepared in the state $|1\rangle$, i.e., the probability amplitude $|a_1|=1$, we can analytically solve the coupled amplitude equations in the steady state and derive the susceptibility $\chi_{\rm p}$ with respect to the probe field according to the induced electric-dipole moment, $P=\varepsilon_0\chi_{\rm p}E_{\rm p}=2N(d_{31}a_3a_1^{*}+d_{41}a_4a_1^{*})$,

$$\begin{aligned}
\chi_{\rm p}&=-\frac{Nd_{31}^2}{\varepsilon_0\hbar}\Big(\chi_{\rm p}^{(1)}+\chi_{\rm p}^{(3)}\Big),\\
\chi_{\rm p}^{(1)}&=\frac{\gamma_4+g_{\rm l}^2\gamma_3-i2g_{\rm l}\gamma_{43}}{\gamma_{43}^2+\gamma_3\gamma_4},\\
\chi_{\rm p}^{(3)}&=\frac{\Omega_{\rm c}^2}{\gamma_2\Big(\gamma_{43}^2+\gamma_3\gamma_4\Big)}\\
&\quad\times\left[\frac{\Big(\gamma_4+g_{\rm l}^2\gamma_3-i2g_{\rm l}\gamma_{43}\Big)\Big(\gamma_4+g_2^2\gamma_3-i2g_2\gamma_{43}\Big)}{\gamma_{43}^2+\gamma_3\gamma_4}\right.\\
&\quad\left.-(g_{\rm l}-g_2)^2\right],
\end{aligned}\tag{2}$$

where $\chi_{\rm p}^{(1)}$ ($\chi_{\rm p}^{(3)}$) is the linear (third-order nonlinear) probe susceptibility, N is the atomic density, $\gamma_2=i\gamma_{21}+(\Delta_p-\Delta_c)$, $\gamma_3=i\frac{\Gamma_{31}+\Gamma_{32}}{2}+(\Delta_p+\Delta)$, and $\gamma_4=i\frac{\Gamma_{41}+\Gamma_{42}}{2}+(\Delta_p-\Delta)$. Interestingly enough, the linear susceptibility is independent of the control field detuning $\Delta_{\rm c}$.

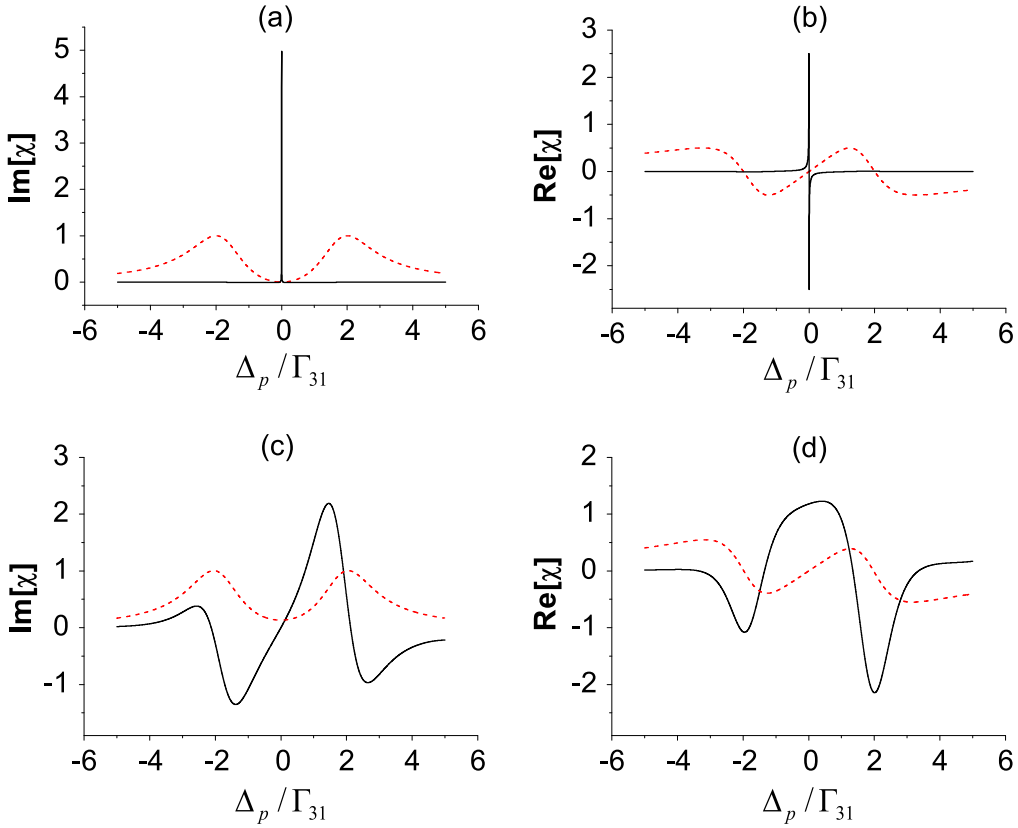

Figure 2. Absorptive (a), (c) and refractive (b), (d) parts of $\chi^{(1)}$ (red dashed curves) and $\chi^{(3)}$ (black solid curves) versus the probe detuning Δ_p in the cases of resonant (a), (b) and off-resonant (c), (d) atom-control field interaction. The other parameters are $\gamma_{21} = 0.002\Gamma_{31}$, $\Delta = 2\Gamma_{31}$, and $p_1 = p_2 = 1$.

From equation (2) we know that the linear probe susceptibility vanishes at the detuning

$$\Delta_p = \frac{1 - g_1^2}{1 + g_1^2}\Delta \tag{3}$$

as

$$\Gamma_{41} = g_1^2\Gamma_{31},\ \Gamma_{42} = g_1^2\Gamma_{32},\ p_1 = p_2 = 1. \tag{4}$$

Then the third-order nonlinear susceptibility reduces to

$$\chi_p^{(3)} = \frac{-(g_1 - g_2)^2}{\gamma_2\left(\gamma_{43}^2 + \gamma_3\gamma_4\right)}\Omega_c^2. \tag{5}$$

Obviously, the nonlinearity susceptibility with respect to the probe field indeed results from the inherent quantum interference. If $g_1 g_2 < 0$ the nonlinear susceptibility is enhanced. In contrast to the EIT schemes for enhanced nonlinearity [23–25], no additional coupling fields are required now. To see the behaviors of linear and third-order nonlinear susceptibilities, we present in figure 2 their spectra with the parameters fulfilling equation (5) for the maximum third-order nonlinearity, that is, $g_1 = -g_2 = 1$ and $\Gamma_{42} = \Gamma_{32} = \Gamma_{41} = \Gamma_{31}$. Specifically, figures 2(a), (b) are plotted for the resonant control field $\Delta_c = 0$ and $\Omega_c = 0.1\Gamma_{31}$. It is seen that the third-order susceptibility in the small region centered at resonance $\Delta_p = 0$ is much stronger than the linear susceptibility, no matter where the latter is located in the spectrum. Figures 2(c), (d) are plotted for the off-resonant control field $\Delta_c = 6\Gamma_{31}$ and $\Omega_c = 3\Gamma_{31}$. Now the region where the third-order susceptibility is dominated over its linear counterpart enlarges significantly. In fact, because it is proportional to Ω_c^2, the third-order susceptibility can in principle be made arbitrarily large simply by increasing the control field intensity. In the following, our attention is focused on the case of the probe resonance $\Delta_p = 0$ where the condition of the maximum third-order nonlinearity $g_1 = -g_2 = 1$ is fulfilled.

3. Electromagnetically induced angular Talbot effect

Nonlinear electromagnetically induced grating. Due to the dependence of the strong third-order nonlinear susceptibility on the control field intensity, the periodic modulation of the absorption and refractive index of the atomic medium with respect to the illumination field, i.e., the EIG effect, can be generated by replacing the constant intensity control field with a standing-wave control field, where the latter results from the intersection of two constant intensity fields propagating in the directions symmetrically displaced with respect to z, as shown in figure 3(b). Then the Rabi frequency of the standing-wave control field can be written as $\Omega_c(x) = \Omega_{c0}\cos(\pi x/\Lambda)$. Here the spatial period of the EIG is Λ, which, in principle, can be made arbitrarily larger than the

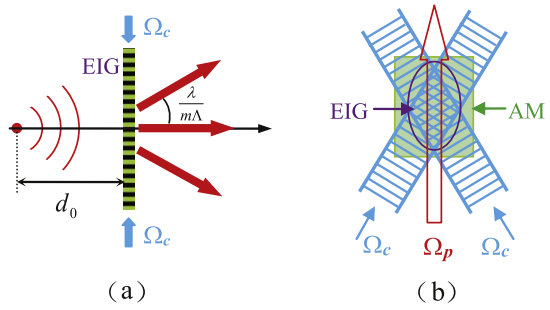

Figure 3. (a) Schematic representation of EIATE of an EIG illuminated by a spherical wave-front, (b) configuration of EIG generation.

wavelength λ of the illumination field by adjusting the angle between the two counterpropagating wave vectors of the control fields. Furthermore, the propagation of the illumination field inside the medium obeys, strictly, the three-dimensional Maxwell's equation, even though it is a plane wave before entering the medium. To focus on the main features of the EIG, we neglect the transverse differential terms of the equation by working in a parameter regime where the atomic density N or Λ is sufficiently large [11]. Then, in the slowly varying envelope approximation, the illumination field on the output surface of the atomic medium ($z = L$) can be obtained, and reads

$$E(x, L) = E(x, 0)\mathrm{e}^{-k\chi_\mathrm{p}''L/2}\mathrm{e}^{ik\chi_\mathrm{p}'L/2}, \tag{6}$$

where $E(x, 0)$ is the illumination field profile before entering the atomic medium, χ_p' (χ_p'') is the real (image) part of the susceptibility, and $k = 2\pi/\lambda$. It is easy to see that the absorption and phase of the illumination field experience periodical modulation as the field passes through the standing wave region. If the system is at resonance $\Delta_\mathrm{p} = \Delta_\mathrm{c} = 0$, $\chi_\mathrm{p} = -\frac{Nd_{31}^2}{\varepsilon_0\hbar}\frac{4}{i\gamma_{21}\Delta^2}\Omega_\mathrm{c}^2(x)$, only the periodic amplitude modulation across the illumination profile is realized, which is the phenomenon reminiscent of an amplitude grating. In other circumstances, phase modulation is introduced, so a hybrid (both amplitude and phase) grating is available. The quantum interference between different atomic decay channels plays a role in the formation of a hybrid grating to enhance Kerr nonlinearity and restrain absorption. Under certain conditions, almost pure phase modulation can be achieved.

Referring to a conventional grating, now the width of a transmission light peak on the output surface of the atomic medium acts equivalently to the spatial extension of a slit of this EIG. As shown by figures 4(a), (b), (c), this peak width is determined by the control parameters of the system. In these figures, only the amplitude EIG case is focused, from which the dependence of its slit width on the parameters can be seen clearly. The tunable property of an EIG may make its application in future possible and easy.

Electromagnetically induced angular Talbot effect. To see the angular Talbot effect of the EIG, as done in the paper [2], we assume that the EIG is illuminated by the field with a parabolic wave front, $E(x, 0) \propto \mathrm{e}^{i\alpha x^2}$, where α defines the curvature of the quadratic phase profile. This wave variation can be induced by illumination with a spherical wave front, ideally generated from a single radiation point on the propagation axis ($x = 0$, $z = -d_0$) as shown in figure 3(a). Then, the relationship $\alpha = \pi/\lambda d_0$ can be easily obtained. Furthermore, because of the periodicity in x/Λ of the illumination susceptibility χ_p, the exponential factor, $\mathrm{e}^{ik\chi L/2}$, in equation (6) can be recast into Fourier series. Thus equation (6) reduces to

$$E(x, L) \propto \mathrm{e}^{i\alpha x^2}\sum_{n=-\infty}^{+\infty} c_n\mathrm{e}^{-iK_n x} \propto \sum_{n=-\infty}^{+\infty} \times c_n\mathrm{e}^{in^2\alpha\Lambda^2}\mathrm{e}^{-iK_n x}, \tag{7}$$

where $c_n = \frac{1}{\Lambda}\int_0^\Lambda \mathrm{e}^{-k\chi_\mathrm{p}''L/2}\mathrm{e}^{ik\chi_\mathrm{p}'L/2}\mathrm{e}^{iK_n x}\mathrm{d}x$ with $K_n = 2\pi n/\Lambda$ ($n = 1, 2, \ldots$), defining the nth complex component of the transmission amplitude in the frequency domain. The latest approximation in equation (7) is valid if the transversal extension of the individual slit is sufficiently short [26].

Evidently, the spherical illumination introduces the additional phase modulation. Following the treatment of [26], as the condition of the discrete phase-modulation shift, or the angular Talbot condition, $\alpha\Lambda^2 = \pi\frac{s}{m}$, is satisfied, where s, m (=1, 2, 3, $\cdots$) are any two coprime integers, the angular spectrum of the diffracted wave can be obtained. It reads

$$\mathcal{E}(k_x) = \mathrm{FT}\{E(x, L)\} \propto \sum_{q=-\infty}^{+\infty} c_q\mathcal{E}_q\left(k_x - q\frac{K_0}{m} - h\frac{K_0}{2m}\right), \tag{8}$$

where coefficient c_q has the same definition as c_n in equation (7) except for their subscript symbols being different, FT stands for Fourier transform, and $\mathcal{E}_q$ is the qth component of the Fourier transform of the complex envelope of the EIG. From equation (8) we can see the typical features of an angular Talbot spectrum that has been seen in the conventional grating case [2]. That is, $h = 1(0)$ if the product sm is an odd (even) number, where $m = 1$ ($m > 1$) corresponds to the integer (fractional) angular Talbot phenomenon. In the spherical wave-front implementation depicted in figure 3(a), the location ($z = -d_0$) of the focal point of the spherical beam becomes $d_0(s; m) = \frac{m}{s}z_T$, where $z_T = \frac{\Lambda^2}{\lambda}$ is referred to as the fundamental Talbot length. The qth-order diffraction is characterized by angle ϕ_q defined as $\sin\phi_q = q\frac{\lambda}{m\Lambda} + h\frac{\lambda}{2m\Lambda}$ and the periodic angular spacing, $\frac{\lambda}{m\Lambda}$. The integer and fractional Talbot phenomena can be observed on the angular spectrum of the wave amplitude, depending on the combination of values of the parameters s and m. In the following, we will verify numerically the existence of a nonlinear EIG and its angular Talbot phenomena.

As discussed above, an amplitude EIG appears as the system is at resonance. Figures 5(a), (b) show respectively the amplitude ($|E(x, L)|$) and the phase (Φ) of the illumination field on the output surface of the atomic medium, where the transversal extension of the whole EIG is large enough. The amplitude of the illumination light varies periodically across the light profile and the phase is fixed, thus it is indeed an amplitude-type of EIG. Figure 5(c) presents the angular

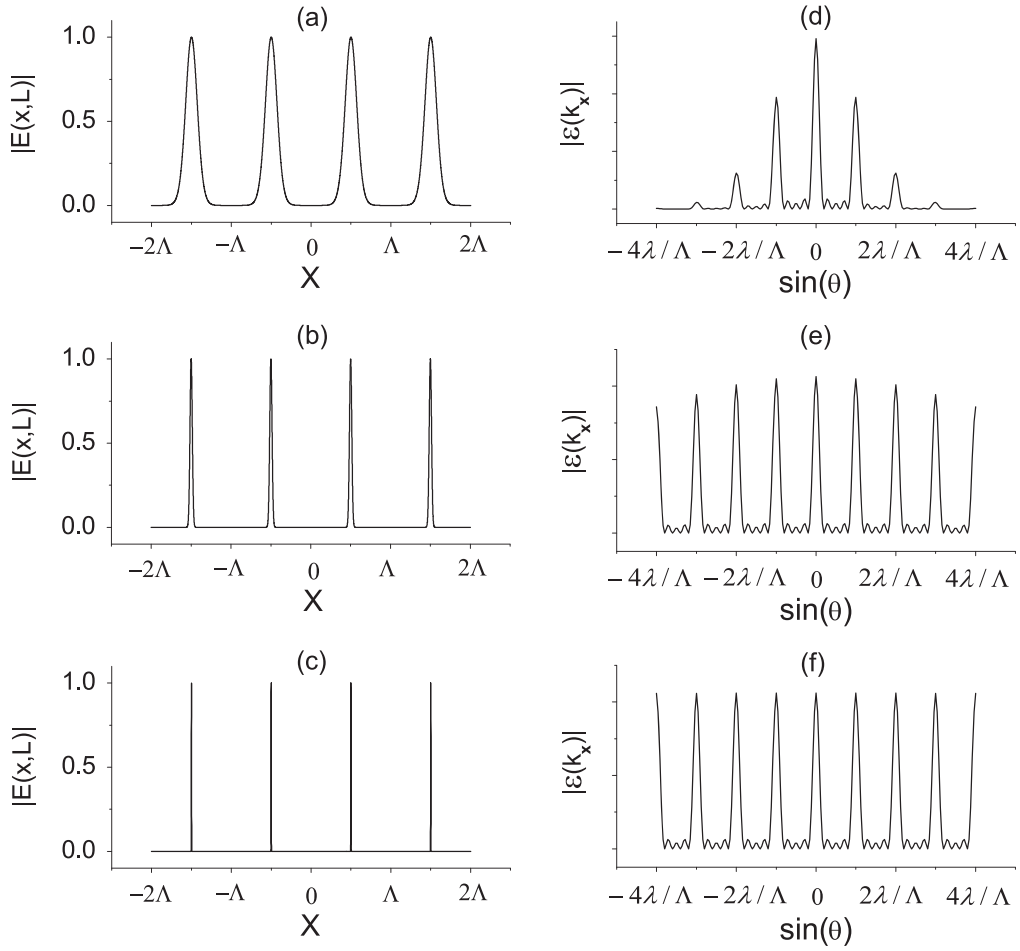

Figure 4. Output profile of illumination field $E(x, L)$ (a), (b), (c) as a function of x and their corresponding diffraction patterns (d), (e), (f) via diffraction angle $\sin(\theta)$ with $\Omega_{c0} = 0.2\Gamma_{31}$, $\Delta = 20\Gamma_{31}$; $\Omega_{c0} = \Gamma_{31}$, $\Delta = 20\Gamma_{31}$; $\Omega_{c0} = \Gamma_{31}$, and $\Delta = 2\Gamma_{31}$. Other parameters are the same as in figure 2.

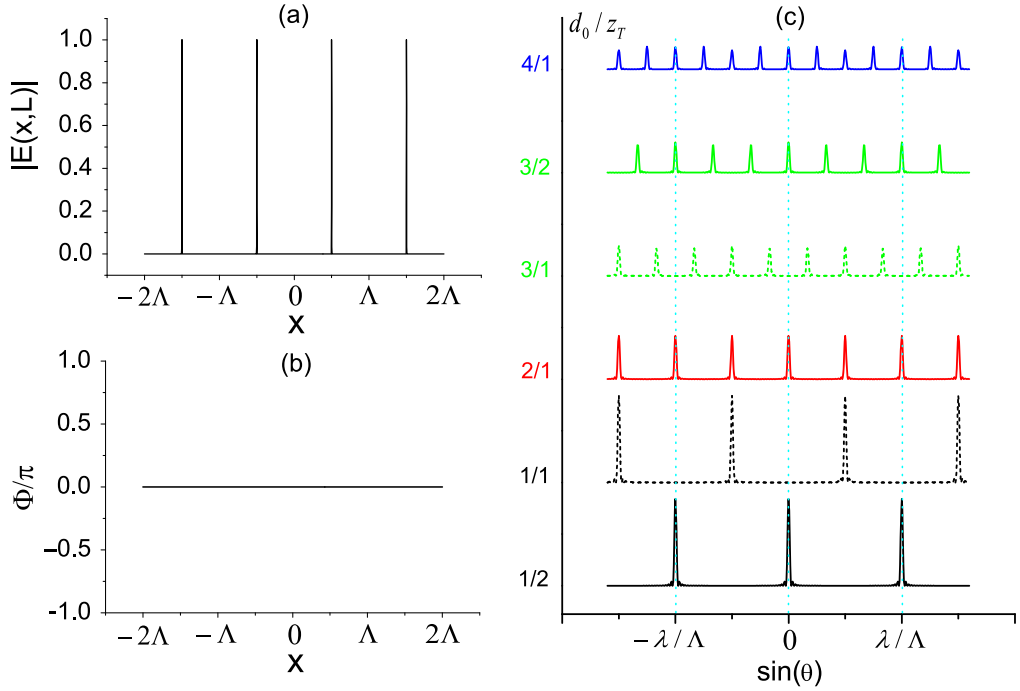

Figure 5. Amplitude (a) and phase (b) of illumination field on output surface of atomic medium, (c) angular diffraction patterns of amplitude EIG with different values of d_0/z_T. $\Omega_{c0} = \Gamma_{31}$ and $\Delta_c = 0.0$. Other parameters are the same as in figure 2.

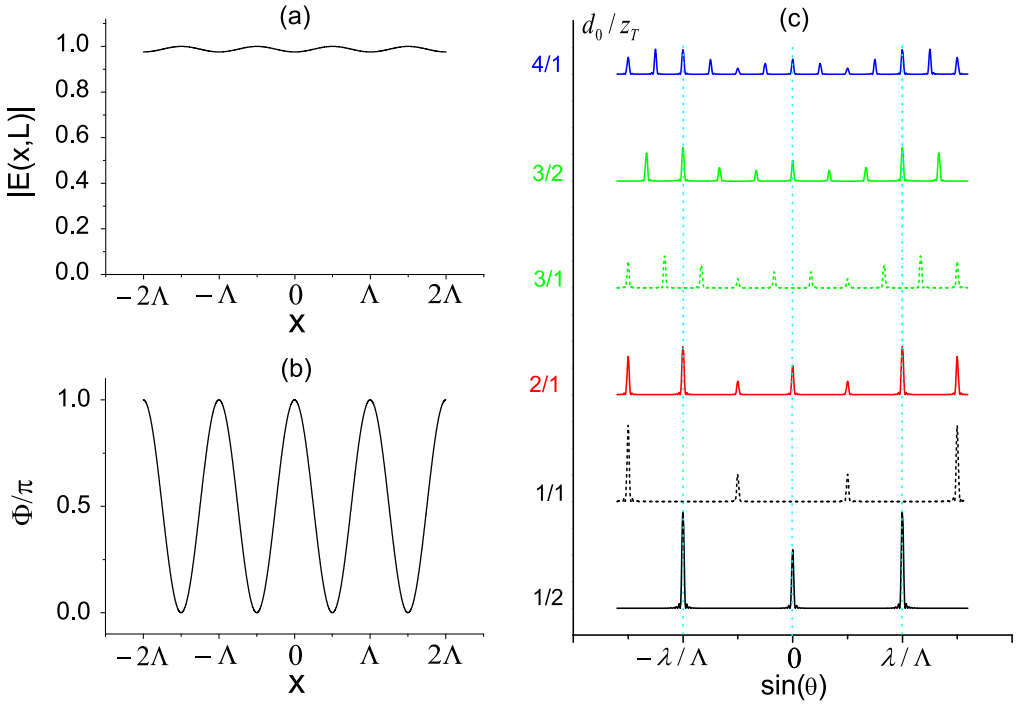

Figure 6. Amplitude (a) and phase (b) of illumination field on output surface of atomic medium, (c) angular diffraction patterns of hybrid EIG with different values of d_0/z_T. $\Omega_{c0} = \Gamma_{31}$ and $\Delta_c = 2\Gamma_{31}$. Other parameters are the same as in figure 2.

diffraction patterns of this amplitude EIG as the function of diffraction angle $\sin(\theta)$ with different source focal point locations normalized by d_0/z_T. The typical features of the angular distribution of this diffraction can be seen clearly. That is, the angular spacing of the EIATE for $m = 1$ (integer EIATE) is larger than that of the EIATE for $m > 1$ (fractional EIATE). For a given m, the periodic angular spacing is fixed, and the angular diffraction pattern with sm being odd is the same as that with sm being even, but shifted by half the angular spacing $\frac{\lambda}{2m\Lambda}$. It can also be seen that the diffraction intensities along different angular directions are almost the same. This is because under our parametric condition, the effective slit width is much smaller than the grating period and, of course, the whole grating scale, and the angular spectrum of a single slit diffraction is very wide. On the other hand, the angular spacing between two diffraction peaks is fixed as the Λ and λ are given. Therefore, it is not easy to observe the intensity difference between two peaks located in the central bright fringe of single slit diffraction. This analysis has been testified by the numerical simulation shown in figures 4(d), (e), (f). Another apparent feature of EIATE is that, as required by the energy conservation law, the individual diffraction intensity decreases as the slit width decreases or as the distance between the focal point of the spherical beam and EIG increases.

A hybrid EIG is available as the system is at off-resonance. Figures 6(a), (b) are plotted for $\Delta_p = 0$, $\Delta_c = 2\Gamma_{31}$, where the periodic modulation with respect to the amplitude and phase of the illumination field can be seen clearly. Evidently, it is a hybrid type of EIG, but the phase modulation effect is much stronger than the amplitude modulation effect. We note here that the phase modulation due to the off-resonant atom–light interaction is reflected by the coefficient c_q, while the phase modulation due to the spherical illumination is considered in the process of deriving angular diffraction spectrum, equation (8). Figure 6(c) shows the angular diffraction patterns of this hybrid EIG. The diffraction patterns spread in a way which is generally similar to its amplitude EIG counterpart. The difference between them is that for a hybrid EIG, the diffraction intensity is angle-dependent, distributing symmetrically about the zero-order diffraction, and the strongest diffraction peak will move from a lower diffraction order to a high one as m increases. This is due to the coaction of the amplitude and the phase modulations in the hybrid EIG, where the amplitude modulation tends to gather light energy to the center of the spectrum (zero-order diffraction) and the phase modulation tends to transfer the light energy to high-order diffraction. Further numerical simulation shows that, in the integer EIATE case of an almost pure phase grating, the first-order diffraction efficiency approaches 34%, the maximum value obtainable in the case of an ideal sinusoidal phase grating [27].

We know from the comparison between equation (8) and equation (7) of [2] that the pattern of angular Talbot spectra should be unique, that is, all diffraction spectra depend on coprime integers m and s in a common way. Their difference, as has been analyzed previously, lies in the details of the spectra. For instance, for given m and s, the angular diffraction intensity obtained with a hybrid EIG varies in a way different from that with a conventional grating. The reason for this is attributed to the peculiar working mechanism of our EIG.

4. Conclusions

In the paper, we have studied the possibility of the angular Talbot effect occuring in a medium that has no macroperiodic structure itself. EIG could be such a kind of medium. We obtain an EIG based on the periodically modulated susceptibility due to the third-order nonlinear effect of a double Λ-type four-level atomic system. One of advantages of this scheme is that the nonlinear susceptibility results from the inherent quantum interference in a multilevel atomic system without using additional lasers and is very strong. Another is that the period of the EIG and the width of its slit can be achieved on demand by adjusting the coherently driven lasers without the need for any physical processing. We have shown the angular Talbot effect of an amplitude EIG, as well as a hybrid EIG, as the condition of the discrete phase-modulation shift of the illumination light front is satisfied. In the latter case, the additional phase modulation due to the off-resonant atom–light interaction affects the angular diffraction intensity. EIG parameters are tunable and the EIG-based angular Talbot effect may have the same potential applications that its periodic grating counterpart is believed to have.

Acknowledgments

This research was supported by National Natural Science Foundation of China, Project Nos. 11447156, 11174040 and 11174038, and by Natural Science Foundation of Shandong Province, Project No. ZR2014AP006.

References

[1] Talbot H F 1836 *Philos. Mag.* **9** 401
[2] Azaña J and Chatellus H G 2014 *Phys. Rev. Lett.* **112** 213902
[3] Patorski K 1989 *Progress in Optics* ed E Wolt vol 27 (Amsterdam: North-Holland) 1–108
[4] Chapman M S, Ekstrom C R, Hammond T D, Schmiedmayer J, Tannian B E, Wehinger S and Pritchard D E 1995 *Phys. Rev.* A **51** R14
[5] Wu S J, Su E and Prentiss M 2007 *Phys. Rev. Lett.* **99** 173201
[6] Li K, Deng L, Hagley E W, Payne M G and Zhan M S 2008 *Phys. Rev. Lett.* **101** 250401
[7] Brezger B, Hackermüller L, Uttenthaler S, Petschinka J, Arndt M and Zeilinger A 2002 *Phys. Rev. Lett.* **88** 100404
[8] Weitkamp T, Nöhammer B, Diaz A and David C 2005 *Appl. Phys. Lett.* **86** 054101
[9] Pfeiffer F, Bech M, Bunk O, Kraft P, Eikenberry E F, Brönnimann C, Grünzweig C and David C 2008 *Nature Mater.* **7** 134
[10] Wen J M, Du S W, Chen H Y and Xiao M 2011 *Appl. Phys. Lett.* **98** 081108
[11] Ling H Y, Li Y Q and Xiao M 1998 *Phys. Rev.* A **57** 1338
[12] Mitsunaga M and Imoto N 1999 *Phys. Rev.* A **59** 4773
[13] Wu J C and Ai B Q 2015 *J. Phys. B: At. Mol. Opt. Phys.* **48** 115504
[14] Harris S E, Field J E and Imamog˘lu A 1990 *Phys. Rev. Lett.* **64** 1107
[15] Qiu T H, Yang G J and Bian Q 2013 *Euro. Phys. Lett.* **101** 44004
[16] Drampyan R, Pustelny S and Gawlik W 2009 *Phys. Rev.* A **80** 033815
[17] Shahidani S, Naderi M H and Soltanolkotabi M 2013 *Phys. Rev.* A **88** 053813
[18] Zhao S C, Liu Z D and Wu Q X 2010 *J. Phys. B: At. Mol. Opt. Phys.* **43** 045505
[19] Dutta S and Dastidar K R 2012 *Mol. Phys.* **110** 431
[20] Menon S and Agarwal G S 1998 *Phys. Rev.* A **57** 4014
[21] Niu Y P and Gong S Q 2006 *Phys. Rev.* A **73** 053811
[22] Zhao S C, Wu Q X and Gong A L 2014 *Chin. Phys. Lett.* **31** 034206
[23] Schmidt H and Imamoglu A 1996 *Opt. Lett.* **21** 1936
[24] Pack M V, Camacho R M and Howell J C 2006 *Phys. Rev.* A **74** 013812
[25] Yang X, Li S, Zhang C and Wang H 2009 *J. Opt. Soc. Am.* B **26** 1423
[26] Berry M V and Klein S 1996 *J. Mod. Opt.* **43** 2139
[27] Goodman J W 1968 *Introduction to Fourier Optics* (New York: McGraw-Hill)